CAV2021
11th International Symposium on Cavitation
May 10-13, 2021, Daejon, Korea

Coupled Vorticity and Velocity Divergence Equations, Applied to Cavitating 2-D Hydrofoils

[1]Konstantinos Iliopoulos*; [1]Spyros A. Kinnas

[1] *Ocean Engineering Group, The University of Texas at Austin, Austin, TX, USA*

Abstract

In this study, the VIScous Vorticity Equation (VISVE) method is applied to predict flow around 2-D hydrofoils in cavitating conditions. The DIVergence of velocity Equation (DIVE) is added to extend the method to compressible flows and coupled with VISVE to predict partial cavitating flow. The addition of DIVE allowed the method to produce convergent, physically meaningful results over a large range of cavitation numbers. The flow is modeled as a homogenous mixture of vapor and liquid with the vapor volume fraction parameter determining their concentrations inside the volume and an additional transport equation for the vapor volume fraction to predict the partial cavitating flow around 2-D hydrofoils. The VISVE method has been designed to be both spatially compact and numerically efficient in comparison to the commonly used Reynolds Averaged Navier-Stokes (RANS) models. The cavity shapes and pressure distributions, predicted by the present method, are compared against those predicted by RANS, for different cavitation and Reynolds numbers, in laminar flow conditions.

Keywords: vortex method; mixture model; cavitation; hydrofoil

Introduction

The cavitation phenomenon describes the rapid phase change between liquid and vapor that occurs under low pressure conditions. In practice cavitation is a common phenomenon in hydrofoils, pipe flows, liquid pumps and marine propellers where there are significant pressure differentials. Depending on the application, cavitation can be the cause of several detrimental effects including structural failure, corrosion, vibration, noise radiation, and loss of lift/thrust in the case of supercavitation. This study will focus on sheet cavitation, which is very common in the case of marine propellers. Specifically, this type of cavitation is defined as a thin, quasi-steady layer of vapor, occurring near the leading edge of the blade and is partly attached to the surface. Although this work addresses the computational analysis of sheet hydrofoil cavitation, the method is by its nature capable to predict cloud and bubble cavitation.

VISVE method, was first proposed and implemented by Tian and Kinnas [1] for the case of 2-D hydrofoils. The method was later extended in the case of 3-D hydrofoils by Wu and Kinnas [2, 3], as well as cylinders in unidirectional and alternating flow by Li and Kinnas [4]. Moreover, VISVE was recently coupled with turbulence models (OpenFOAM) in the case of wetted flows past a 2-D hydrofoil by Hao and Kinnas [5]. An initial attempt to model cavitation for the 2-D hydrofoil was made by Lu et al [6], with results having good agreement with RANS at high cavitation numbers but deviating significantly at lower cavitation numbers. In this study, the topic of cavitation is revisited in order to improve the mathematical formulation, as well as the employed numerical scheme.

The mixture model is implemented in the case of two-phase cavitating flows, which assumes a homogeneous mixture of liquid and vapor, with different concentrations at every point. The variations in density and dynamic viscosity are proportional to the vapor volume fraction, describing the percentage of vapor at each computational cell. An additional vapor transport equation is added to model the evolution of the cavity. The mass transfer between the two phases is controlled by including appropriate source terms in the vapor transport equation. There are several different models describing the behavior of these sources [7,8,9], based on different assumptions. In this work results from the Zwart-Gerber- Belamri [8] will be presented. On the other hand, in order to capture the inertial characteristics of a compressible flow, the DIVergence of velocity Equation (DIVE) has been added which regulates the magnitude of the source terms.

The goal of this study is to incorporate the mixture model in VISVE to predict the cavitating flow around a hydrofoil. To verify the coupled scheme, the results are compared with those from the commercial RANS solver, *ANSYS/Fluent*.

*Corresponding Author, Konstantinos Iliopoulos: kostas.9302@utexas.edu

Numerical Methods and Models

1. Mass conservation

In the case of the mixture model, both the liquid and vapor phases are considered incompressible. The density (ρ_m) and dynamic viscosity (μ_m) of the mixture are given by the following relation:

$$\rho_m = \alpha\rho_v + (1-\alpha)\rho_l;\ \mu_m = \alpha\mu_v + (1-\alpha)\mu_l \tag{1}$$

where ρ_v, ρ_l is the density of the vapor phase and the liquid phase; μ_v, μ_l is the dynamic viscosity of the vapor phase and the liquid phase. The conservation of mass for the mixture is:

$$\frac{\partial \rho_m}{\partial t} + \vec{\nabla}\cdot(\rho_m\vec{q}) = 0 \tag{2}$$

where $\vec{q}$ is the velocity. In the case of an individual phase the mass conservation requires an additional source term for the mass transfer between phases. In the case of vapor, the conservation of mass may be written as:

$$\frac{\partial(\alpha\rho_v)}{\partial t} + \vec{\nabla}\cdot(\alpha\rho_v\vec{q}) = R \tag{3}$$

where, R is the phase change rate: $R = R_c$ or $R = -R_e$, with R_c, R_e representing condensation rate and evaporation rate, respectively, which can be obtained by the Zwart-Gerber-Belamri model. Equation (3) is also known as the vapor transport equation. Instead of using the mass conservation equation for the liquid, equations (2) and (3) are combined to give the continuity equation of the flow:

$$\vec{\nabla}\cdot\vec{q} = R\left(\frac{1}{\rho_v} - \frac{1}{\rho_l}\right) \tag{4}$$

2. Cavitation model

The phase change rate, R, is calculated using Zwart-Gerber-Belamri's model [8]. This model assumes constant bubble radius and simulates the bubble growth and collapse as:

$$R_e = F_{evap}\frac{3\alpha_{nuc}(1-\alpha)\rho_v}{\Re_B}\sqrt{\frac{2}{3}\frac{(p_v - p)}{\rho_l}} \tag{5}$$

$$R_C = F_{cond}\frac{3\alpha\rho_v}{\Re_B}\sqrt{\frac{2}{3}\frac{(p - p_v)}{\rho_l}} \tag{6}$$

In the above equations, α_{nuc} is the nucleation site volume fraction, F_{evap} and F_{cond} are two empirical calibration coefficients for the evaporation and condensation process, respectively. The default values for the above parameters are as follows: $\alpha_{nuc} = 5.0\times10^{-4}, \Re_B = 1.0\times10^{-6}m,\ F_{evap} = 50,\ F_{cond} = 0.01$. Here, p is the local pressure and p_v is the saturated vapor pressure for the liquid.

3. Pressure Calculation

The first approximation of pressure, p_0, in the case of steady, incompressible flow is given by the momentum equation in the direction, $\vec{n}$, normal to the hydrofoil surface:

$$\frac{\partial p_0}{\partial n} = -\rho\frac{\partial}{\partial n}\left(\frac{1}{2}q^2\right) - \rho(\vec{n}\times\vec{q})\cdot\vec{\omega} - \mu\left(\vec{\nabla}\times\vec{\omega}\right)\cdot\vec{n} \tag{7}$$

Where ρ is density, μ is the dynamic viscosity, $\vec{q}$ is the total velocity, $\vec{\omega}$ is vorticity and μ is dynamic viscosity. Since in VISVE the grid is generated normal to the hydrofoil, a line integral can be conducted along the direction normal to the hydrofoil from the outer boundary to any point (x) within the domain to calculate the pressure at that point. Therefore, as long as the pressure on the outer boundary of the domain is given, the pressure within the whole domain can be obtained.

*Corresponding Author, Konstantinos Iliopoulos: kostas.9302@utexas.edu

$$p(x) = \int_{outer\ boundary}^{x} \frac{\partial p}{\partial n} \cdot d\boldsymbol{n} \tag{8}$$

The pressure at the inlet is calculated using the Bernoulli equation for steady, incompressible, and inviscid flows

$$p_{boundary}(x) = p_\infty + \frac{1}{2}\rho_l(q_\infty^2 - q^2(x)) \tag{9}$$

The total pressure in the case of cavitation is:

$$p := p_0 + p_{cor} \tag{10}$$

where p_{cor} is the pressure correction for the cavitating flow.

4. Divergence of Velocity Equation

Detailed derivations and descriptions of the equations and the numerical methods presented in the next sections, along with grid dependence studies of the results can be found in Iliopoulos [10].

Taking the divergence of the momentum equation we get the DIVergence of velocity Equation (DIVE):

$$\frac{\partial(\vec{\nabla}\cdot\vec{q})}{\partial t} = -\vec{\nabla}\cdot\left(\frac{\vec{\nabla}p_{cor}}{\rho}\right) + \vec{\nabla}\cdot\left[\nu\,\vec{\nabla}(\vec{\nabla}\cdot\vec{q})\right] + Q_{\vec{\nabla}\cdot\vec{q}} \tag{11}$$

where ρ and ν are the density and kinematic viscosity of the mixture, respectively. The last term in the equation is related to the viscous stresses due to the change in density and viscosity near the cavity and are treated explicitly. The expression for $Q_{\vec{\nabla}\cdot\vec{q}}$ is given as function of density, viscosity and velocity gradients [9].

The pressure correction component, p_{cor}, in equation (10) is such that the solution of equation (11) satisfies the continuity equation (4). The divergence of velocity equation is solved iteratively with the pressure correction equation following the SIMPLEC algorithm. Specifically, the solution of DIVE at the and m-th iteration can be written in the following matrix form:

$$A_D\left(\vec{\nabla}\cdot\vec{q}\right)^m + A_{OD}\left(\vec{\nabla}\cdot\vec{q}\right)^m = -\vec{\nabla}\cdot\left(\frac{\vec{\nabla}p_{cor}^m}{\rho}\right) + Q_{\vec{\nabla}\cdot\vec{q}} \tag{12}$$

where $A = A_D + A_{OD}$ is the coefficient matrix of the divergence equation, with A_D being the matrix with the diagonal elements of A and A_{OD} the matrix with the off-diagonal elements.

5. Pressure Correction Equation

The pressure correction equation results from subtracting equation (12) at the (m-1)-th iteration from the same equation at the m-th iteration.

$$A\left(\vec{\nabla}\cdot\vec{q}\right)^m + \vec{\nabla}\cdot\left(\frac{\vec{\nabla}p^m}{\rho}\right) = A\left(\vec{\nabla}\cdot\vec{q}\right)^{m-1} + \vec{\nabla}\cdot\left(\frac{\vec{\nabla}p^{m-1}}{\rho}\right) \tag{13}$$

In the case of the SIMPLEC (Semi-Implicit Method for Pressure Linked Equations Corrected) algorithm, the following linear approximation is used, for the coefficients of the i-th equation:

$$\left(\vec{\nabla}\cdot\vec{q}\right)_i^m \sum_k A_{OD,k} \approx \sum_k A_{OD,k}\left(\vec{\nabla}\cdot\vec{q}\right)_k^m \tag{14}$$

Substituting the above approximation to equation (13) and $\left(\vec{\nabla}\cdot\vec{q}\right)^m$ from the continuity equation we get:

$$\tilde{A}_D\, C^m \sqrt{|p^m - p_v|} + \vec{\nabla}\cdot\left(\frac{\vec{\nabla}p^m}{\rho}\right) = \tilde{A}_D\left(\vec{\nabla}\cdot\vec{q}\right)^{m-1} + \vec{\nabla}\cdot\left(\frac{\vec{\nabla}p^{m-1}}{\rho}\right) \tag{15}$$

where $\tilde{A}_D := A_{D,i} + \sum_k A_{OD,k}$ is the diagonal matrix of the SIMPLEC method. The coefficient C^m, in equation (15) depends on the cavitation model and is defined by the following relation.

*Corresponding Author, Konstantinos Iliopoulos: kostas.9302@utexas.edu

$$\left(\vec{\nabla}\cdot\vec{q}\right)^{m}=\left(\frac{1}{\rho_v}-\frac{1}{\rho_l}\right)R^{m}\ =C^{m}\sqrt{|p^{m}-p_v|} \tag{16}$$

We set the parametric pressure $q^m \coloneqq \sqrt{|p^m - p_v|}$ and keep all the non-linear terms, including C^m at the previous iteration, then the pressure correction equation becomes:

$$-sign(C^{m-1})\,\vec{\nabla}\cdot\left(\frac{2q^{m-1}\vec{\nabla}\delta q^{m}}{\rho}\right)+\tilde{A}_D C^{m-1}\delta q^{m}=\tilde{A}_D\left[\left(\vec{\nabla}\cdot\vec{q}\right)^{m-1}-C^{m-1}q^{m-1}\right] \tag{17}$$

where $\delta q^m := q^m - q^{m-1} = \sqrt{|p^m - p_v|} - \sqrt{|p^{m-1} - p_v|}$. The boundary conditions for δq^m are Dirichlet at the inlet and Neumann on the foil and the outlet.

6. Vorticity Transport Equation

Taking the curl of the momentum equation we get the viscous vorticity equation. In the 2-D case the vorticity becomes a scalar:

$$\frac{\partial\omega}{\partial t}+\vec{\nabla}\cdot(\vec{q}\,\omega)=\vec{\nabla}\times\left(\frac{\vec{\nabla}p}{\rho}\right)+\vec{\nabla}\cdot\left(\nu\vec{\nabla}\omega\right)+Q_\omega \tag{18}$$

The last term in the equation is related to the viscous stresses due to the change in density and viscosity near the cavity and are treated explicitly. The expression for Q_ω is given as function of density, viscosity, and velocity gradients [10]. An alternative method for calculating the residual viscous terms, using the hydrofoil assumption, can be found in [11].

7. Boundary treatment

The boundary condition for DIVE and VISVE are the same, with Dirichlet condition at the inlet and Neumann boundary condition at the outflow and foil. However, the velocities calculated from the vorticity, ω, and the source, $\vec{\nabla}\cdot\vec{q}$, field using the Biot-Savart law will not satisfy the non-slip and non-through boundary condition on the wall. A vorticity creation scheme based on the Boundary Element Method (BEM), shown in Figure 1, is designed to eliminate tangential and normal velocity, denoted as q^n, q^s on the wall. After assigning the newly created vorticity into cells in the first layer, the non-slip boundary condition will be satisfied.

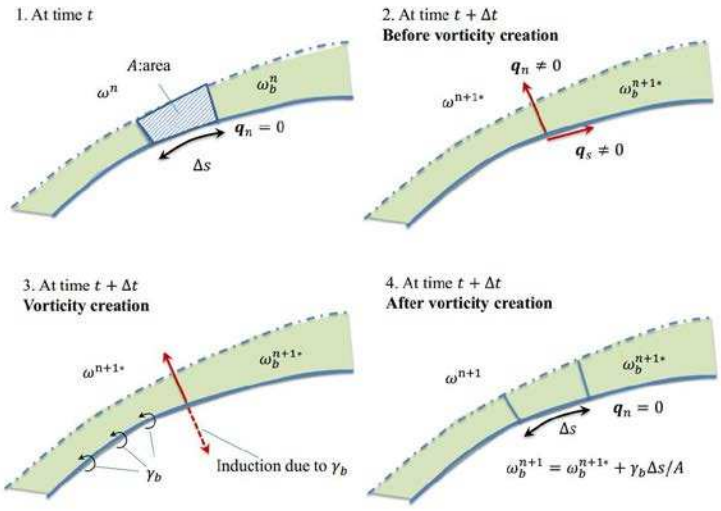

Figure 1: Schematic figure for the vorticity creation algorithm [1]

*Corresponding Author, Konstantinos Iliopoulos: kostas.9302@utexas.edu

Results and comparison with RANS

1. Grid Configurations and numerical setup

The following results are for a NACA66 hydrofoil with 4% thickness to chord length ratio and 1% camber to chord length ratio. The grid configuration in VISVE and RANS are shown in Figure 2 and 3, respectively. The VISVE domain is much more compact with 26,000 cells compared to the 167,000 cells of the RANS domain. In the RANS model, the cavitation was modeled as steady laminar flow, whereas in VISVE the flow was modeled as unsteady with $\Delta t = 0.0001\ s$.

The commercial software ANSYS-FLUENT was used for the RANS cases. PRESTO!, was used for the pressure face interpolation and QUICK for the momentum and vapor transport equations. The gradients were calculated using the Least-squares-cell-based scheme. For the computational results, we use the following non-dimensional parameters:

$$\text{Cavitation Number } \sigma = \frac{p - p_v}{\frac{1}{2}\rho_l {U_\infty}^2} \tag{19}$$

$$\text{Reynolds Number } Re = \frac{U_\infty L}{\nu_l} \tag{20}$$

The Zwart-Gerber-Belamri's bubble radius is set to $R_B = 10^{-5}$m and the angle of attack (AOA) to 4^o. For the first four cases the Reynold's number is $Re \approx 4800$ which corresponds to a laminar flow regime. The results of a wetted case $\sigma = 1.6$ and cavitation cases of $\sigma = 1.2$, $\sigma = 1.0$ and $\sigma = 0.8$ are presented next.

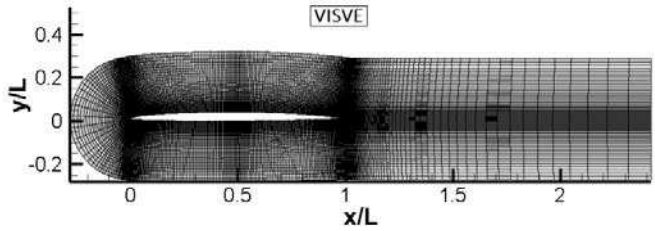

Figure 2: VISVE computation domain and grid configuration (26,000 cells)

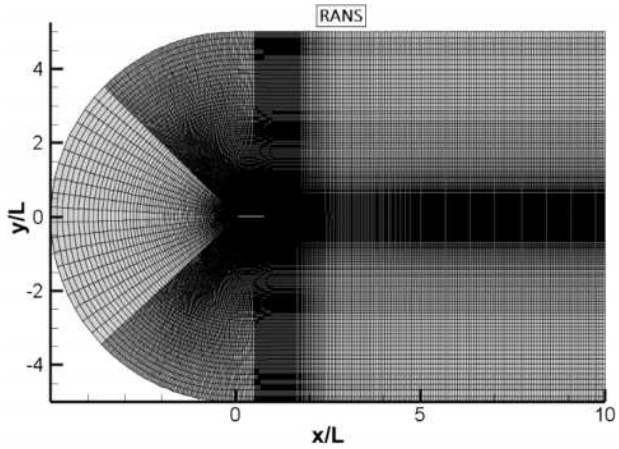

Figure 3: RANS computation domain and grid configuration (167,000 cells)

*Corresponding Author, Konstantinos Iliopoulos: kostas.9302@utexas.edu

2. Wetted case ($\sigma > 1.6$)

Since cavitation is a pressure-driven phenomenon, it is important to validate the pressure coefficient predicted from the wetted cases before we go into cavitating flow. The pressure coefficient predicted by VISVE and RANS are compared in Figure 4. The two models yield very close profiles to each other. The good correspondence verifies the reliability of VISVE model in fully wetted cases.

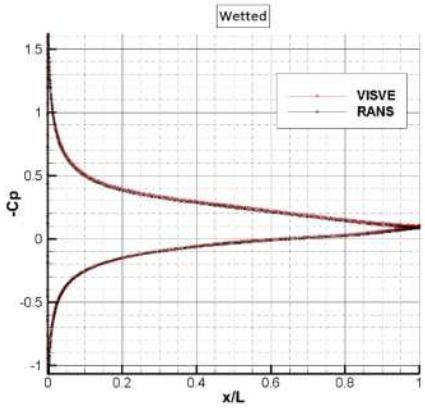

Figure 4: Comparison of pressure coefficient distribution on the hydrofoil predicted from VISVE and RANS at $Re = 4800$, and $\sigma = 1.6$ (wetted)

3. Cavitation at $Re = 4800$

The cavitating results shown below were simulated using the Zwart-Gerber-Belamri's model. The pressure coefficients and the cavity shape at $\sigma = 1.2$, $\sigma = 1.0$ and $\sigma = 0.8$ are shown in Figure 5-11. There is a distinct difference in the pressure coefficient between the VISVE and RANS results, especially for lower cavitation numbers. This might be attributed to the fact that in VISVE both the baroclinic torque, $\vec{\nabla} \times (\vec{\nabla} p/\rho)$, and the residual viscous terms, Q_ω, are neglected.

It is worth noting that the pressure underneath the cavity is not constant. Indeed, cavitation models based on the Rayleigh-Plesset equation require pressures lower than vapor pressure for cavitation inception to occur.

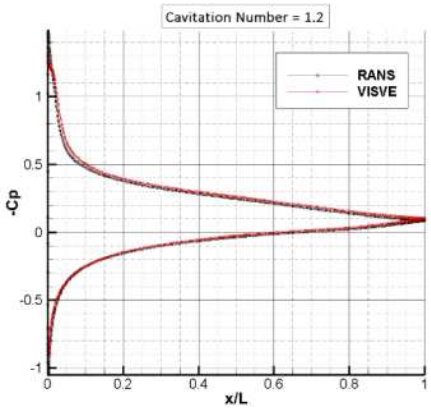

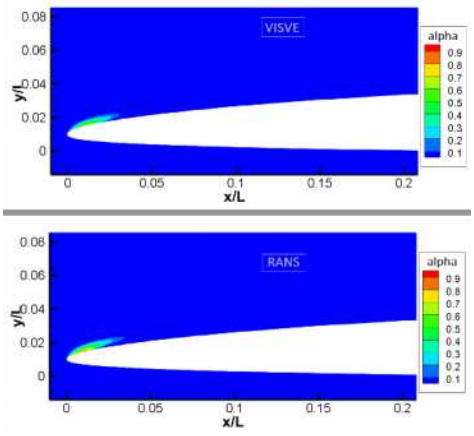

*Corresponding Author, Konstantinos Iliopoulos: kostas.9302@utexas.edu

Figure 6: Pressure coefficient comparison between VISVE and RANS at Re= 4,800 $\sigma = 1.2$

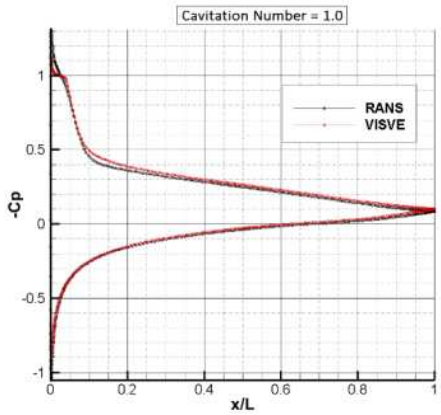

Figure 7: Vapor fraction contour comparison between VISVE and RANS at Re= 4,800 $\sigma = 1.2$

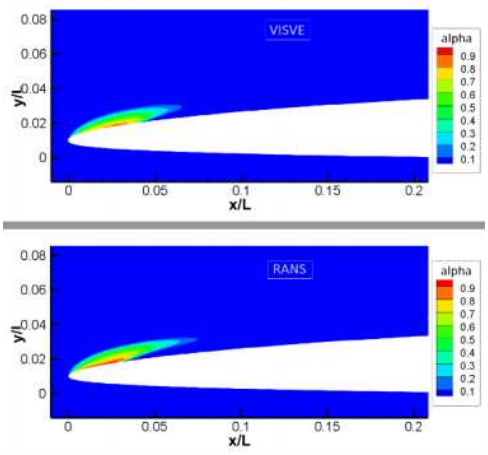

Figure 8: Pressure coefficient comparison between VISVE and RANS at Re= 4,800 $\sigma = 1.0$

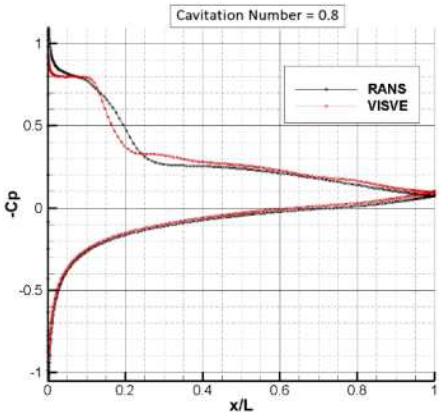

Figure 9: Vapor fraction contour comparison between VISVE and RANS at Re= 4,800 $\sigma = 1.0$

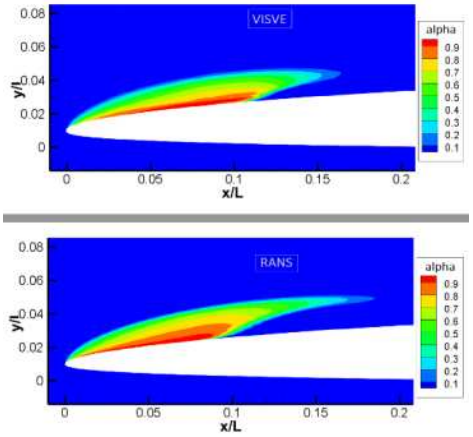

Figure 10: Pressure coefficient comparison between VISVE and RANS at Re= 4,800 $\sigma = 0.8$

Figure 11: Vapor fraction contour comparison between VISVE and RANS at Re= 4,800 $\sigma = 0.8$

4. Cavitation at $Re = 2500$

In the case of cavitation number $\sigma = 0.8$, we include the results for $Re = 2500$ to examine the effects of Reynolds number on the cavity. Results from VISVE and RANS are shown in Figures 12 and 13. In particular, it is evident that viscosity affects the size of the cavity. VISVE seems to underestimate the maximum value for the vapor volume fraction, resulting in a smaller cavity. The differences are more visible in the shown pressure distributions in Figure 13.

Conclusions and Future Work

An improved numerical model which couples our VIScous Vorticity Equation (VISVE) model with a mixture model to simulate cavitating flow around hydrofoils is proposed and the predicted velocity, vorticity, pressure and cavity patterns are compared with those from Reynold Averaged Navier-Stokes (RANS) simulations. The addition of an equation for the divergence of the velocity vector combined with an improved numerical algorithm for the solution of the resulting nested equations was found to improve the results of the method significantly over those of an older version of the method. In fully wetted conditions, the VISVE model predicts pressure distributions which are very

*Corresponding Author, Konstantinos Iliopoulos: kostas.9302@utexas.edu

close to those predicted from RANS. In the cases of moderate cavitation number ($\sigma = 1.2$, $\sigma = 1.0$), VISVE predicts pressures and cavity shapes which are comparable to those from RANS. With lower cavitation number, $\sigma = 0.8$, VISVE predicts smaller cavity extent than that from RANS, especially for smaller Re numbers. Further efforts will be made in the near future to resolve the differences in the cavity size predicted by the present method and by RANS. In the future, the authors intend to include the effects of turbulence into their method, as well as extend it in the case of cavitating 3-D hydrofoils and ultimately propeller blades.

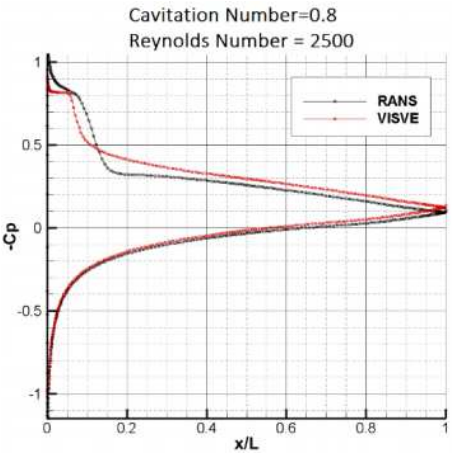

Figure 12: Pressure coefficient comparison between VISVE and RANS at Re= 2,500 $\sigma = 0.8$

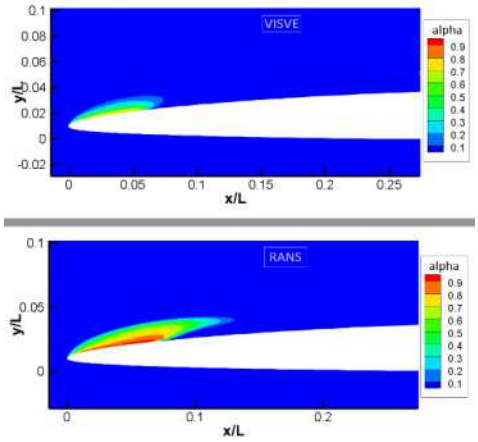

Figure 13: Vapor fraction contour comparison between VISVE and RANS at Re= 2,500 $\sigma = 0.8$

Acknowledgement

Support for this research was provided by the U.S. Office of Naval Research (Grant Nos. N00014-14-1-0303 and N00014-18-1-2276; Dr. Ki-Han Kim) partly by Phase VIII of the "Consortium on Cavitation Performance of High Speed Propulsors".

References

[1] Tian, Y., Kinnas, S.A.: A Viscous Vorticity Method for Propeller Tip Flows and Leading Edge Vortex. In: Symposium on Marine Propulsors (2015).
[2] Wu, C. and Kinnas, S.A., "A 3-D VIScous Vorticity Equation (VISVE) Method Applied to Flow Past a Hydrofoil of Elliptical Planform and a Propeller", 6th Symposium on Marine Propulsors, smp'19, May 26-30, 2019, Rome, Italy.
[3] Wu, C. and Kinnas, S.A., (2020) "Parallel Implementation of a VIScous Vorticity Equation (VISVE) Method in 3-D Incompressible Flow", Journal of Computational Physics, 109912.
[4] Li, Z., Kinnas, S.A.: VISVE , a Vorticity Based Model Applied to Unidirectional and Alternating Flow around a Cylinder. In: 22th SNAME Offshore Symposium, Houston, Texas, USA (2017).
[5] Yao, H. and Kinnas, S.A. (2019). Coupling Viscous Vorticity Equation (VISVE) Method with OpenFOAM to Predict Turbulent Flow around 2-D Hydrofoils and Cylinders, 29th International Symposium on Ocean and Polar Engineering (ISOPE) conference, Honolulu, Hawaii, USA, June 16-21.
[6] Xing, L., Wu, C., and Kinnas, S.A. (2018). VISVE, a Vorticity Based Model Applied to Cavitating Flow around a 2-D Hydrofoil, 10th International Symposium on Cavitation, Baltimore, Maryland, USA.
[7] Schnerr, G.H. and Sauer, J., "Physical and Numerical Modeling of Unsteady Cavitation Dynamics", In Fourth International Conference on Multiphase Flow, New Orleans, USA. 2001.
[8] Zwart, P.J, Gerber, A.G., and Belamri, T., "A Two-Phase Flow Model for Predicting Cavitation Dynamics", In Fifth International Conference on Multiphase Flow, Yokohama, Japan. 2004.
[9] Singhal, A.K., Li, H.Y., Athavale, M.M., and Jiang Y.,"Mathematical Basis and Validation of the Full Cavitation Model", ASME FEDSM'01. New Orleans, Louisiana 2001.
[10] Iliopoulos, K., "VISVE, a Vorticity Based Model Applied to 2-D Hydrofoils in Cavitating Conditions", MS thesis, Ocean Engineering Group, The University of Texas at Austin, August 2020.
[11] Kinnas, S.A. VIScous Vorticity Equation (VISVE) for Turbulent 2-D Flows with Variable Density and Viscosity. J. Mar. Sci. Eng. 2020, 8, 191.

*Corresponding Author, Konstantinos Iliopoulos: kostas.9302@utexas.edu